PROTEINS: Structure, Function, and Genetics 45:382–396 (2001)

Helix-Coil Transition of PrP106–126: Molecular Dynamic Study

Yaakov Levy,[1*] Eilat Hanan,[2] Beka Solomon,[2] and Oren M. Becker[1†]
[1]*Department of Chemical Physics, School of Chemistry, Tel Aviv University, Ramat Aviv, Tel Aviv, Israel*
[2]*Department of Molecular Microbiology and Biotechnology, George S. Wise Faculty of Life Science, Tel Aviv University, Ramat Aviv, Tel Aviv, Israel*

ABSTRACT **A set of 34 molecular dynamic (MD) simulations totaling 305 ns of simulation time of the prion protein-derived peptide PrP106–126 was performed with both explicit and implicit solvent models. The objective of these simulations is to investigate the relative stability of the α-helical conformation of the peptide and the mechanism for conversion from the helix to a random-coil structure. At neutral pH, the wild-type peptide was found to lose its initial helical structure very fast, within a few nanoseconds (ns) from the beginning of the simulations. The helix breaks up in the middle and then unwinds to the termini. The spontaneous transition into the random coil structure is governed by the hydrophobic interaction between His^{111} and Val^{122}. The A117V mutation, which is linked to GSS disease, was found to destabilize the helix conformation of the peptide significantly, leading to a complete loss of helicity approximately 1 ns faster than in the wild-type. Furthermore, the A117V mutant exhibits a different mechanism for helix-coil conversion, wherein the helix begins to break up at the C-terminus and then gradually to unwind towards the N-terminus. In most simulations, the mutation was found to speed up the conversion through an additional hydrophobic interaction between Met^{112} and the mutated residue Val^{117}, an interaction that did not exist in the wild-type peptide. Finally, the β-sheet conformation of the wild-type peptide was found to be less stable at acidic pH due to a destabilization of the His^{111}–Val^{122}, since at acidic pH this histidine is protonated and is unlikely to participate in hydrophobic interaction. Proteins 2001;45:382–396.** © 2001 Wiley-Liss, Inc.

Key words: prion protein; PrP106–126; A117V mutation; helix-coil transition

INTRODUCTION

Prion diseases, such as scrapie of sheep and goats, bovine spongiform encephalopathy, and Creuzfeldt–Jacob disease (CJD) and Gerstmann–Sträussler–Scheinker disease (GSS) of humans, are characterized by the accumulation of abnormal forms of the prion protein, termed PrP^{SC}, in the brain.[1,2] In contrast with the normal cellular prion protein (PrP^{C}), PrP^{SC} is partly resistant to protease digestion and has a marked tendency to form insoluble aggregates of amyloid fibrils.[3,4] The accumulation of PrP^{SC} as PrP amyloid in the brain is thought to be responsible for the nerve cell degeneration.[5]

Nuclear magnetic resonance (NMR) studies of recombinant murine PrP indicate that the normal protein is composed of two structurally distinct moieties: an extended N-terminus segment (residue 23–125) with features of a flexibly disordered polypeptide chain, and a well-defined globular domain (residue 126–231) with three α-helices and a two-stranded anti-parallel β-sheet.[6,7] Although the precise nature of the PrP^{C} to PrP^{SC} transition remains unclear, there is certainly a striking conformational change, with a decrease in α-helical secondary structure (from 42–30%) and a remarkable increase in β-sheet content (from 3–43%).[8,9] This rearrangement is accompanied by the acquisition of abnormal physicochemical properties, including insolubility in nondenaturing detergents and partial resistance to digestion.

Secondary structure prediction based on the prion protein sequence suggested that the prion protein is composed of four α-helical regions, designated H1–H4.[10] However, NMR studies have shown that, in fact, the H1 region (residues 109–122) does not adopt an α-helix configuration, and that the prion protein contains only three α-helix regions.[6,11–13] Further, experimental studies using a peptide corresponding to the H1 region of PrP have shown that the peptide has low solubility in water, forming β-sheets, which polymerize into fibrils.[14–16] In organic solvents, the same peptide adopts a metastable α-helical structure that reverts to an extended conformation when exposed to water vapor.[11] According to crystallographic measurements, the β-sheet conformation of the peptide that corresponds to the H1 region is stabilized by hydrophobic interaction between His^{111} and Ala^{117}.[17] This interaction can explain how a replacement of Ala^{117} by the more hydrophobic Val results in a more stable folded conformation at neutral pH, since valine may strengthen this interaction, thus facilitating the folding of H1. By contrast, at acidic pH, this replacement produces an extended conformation.[17] This effect is attributable to the protonation of histidine at acidic pH, which adds a positive charge

†Oren Becker's current address is, Bio Information Technologies (Bio-I.Y.) Ltd., 3 Hayetzira St., Ramat Gan 52521, Israel

*Correspondence to: Y. Levy, School of Chemistry, Tel-Aviv University, Tel-Aviv, 69978, Israel. E-mail: kobylevy@post.tau.ac.il

Received 8 December 2001; Accepted 12 June 2001

to this residue, making it unlikely to participate in a hydrophobic interaction.

Like the H1 fragment (PrP109–122), the larger PrP106–126 peptide also possesses similar structural characteristics in terms of hydrophobic interactions. Previous studies have shown that a synthetic peptide homologous of residues 106–126 of human PrP (PrP106–126) exhibits some of the pathogenic and physicochemical properties of PrP^{SC}.[5,18–20] This peptide shows a remarkable conformational polymorphism, acquiring different secondary structures in different environments.[20] In general, in buffered solutions this peptide tends to adopt a β-sheet conformation and to aggregate into amyloid fibrils that are partly resistant to digestion with protease. These findings suggest that the PrP region, including residues 106–126, may be the key region in which the global conformational change of the protein from PrP^{C} to PrP^{SC} is initiated. This notion is supported by the fact that deletion of residues 23–88 does not prevent the conversion of PrP^{C} to PrP^{SC}, whereas the ablation of residues 108–121 or 122–140 together with residues 23–88 prevents this process.[21] In addition, the observation that the N-terminus part of PrP (residues 23–125) is highly flexible and is more susceptible to structural transitions than the C-terminus globular domain also supports this hypothesis.

In recent years, many properties of the PrP106–126 and its variants, including physicochemical properties, secondary structure contents, and fibrillogenic propensity, have been studied under different chemical conditions (pH, ionic strength, and a membrane-like environment).[22,23] The conformational polymorphism, as well as the fibrillogenic properties of PrP106–126, were hypothesized to be related, at least in part, to the His^{111}. To test this hypothesis and to establish the importance of residue 111 for amyloid formation, several mutations were introduced at this position. In particular, to test whether the amyloid is formed via hydrophobic interactions, in which the histidine is presumed to take part, a hydrophobic residue (alanine), instead of the histidine, was introduced.[22] This replacement did indeed lead to higher β-sheet content and similar aggregation propensity. Furthermore, because the fibrillogenic propensity decreases in acidic pH, the histidine was also replaced by another ionizable residue, lysine.[22] In general, the latter replacement led to a decrease in both the β-sheet content and the aggregation propensity.

Another residue, in addition to His^{111}, that is implicated as taking part in the PrP106–126 amyloid formation is Ala^{117}. This hypothesis is supported by the fact that a substitution of alanine by valine at position 117 is linked to GSS disease,[2] possibly by favoring the β-sheet conformation over the α-helical conformation. In fact, a previous molecular dynamics (MD) study of the H1 peptide in water by Kazmirski et al.[24] showed that, of a variety of replacements of Ala^{117} with hydrophobic amino acid residues, only the Val^{117} substitution resulted in helix destabilization. Furthermore, a crystallographic study of H1 in the β-sheet structure by Inouye and Kirschner[17] showed that His^{111} indeed faces Ala^{117}. These researchers suggested that because of the stronger hydrophobic interactions between His and Ala, a replacement of Ala by Val may facilitate the formation of a H1 β-sheet. Recent circular dichroism (CD) spectroscopy measurement of PrP106–126 by Salmona et al.[22] was interpreted as an indication that the presence of Val at position 117 increases the aggregation properties of the amidated peptide. While this substitution had no significant effect on the spectral features and structural stability of PrP106–126, it did show that the degree of β-sheet secondary structures of an amidated peptide with this substitution is larger compared with the wild-type amidated peptide.

Salmona et al. suggested another possible model of the β-sheet formation by PrP106–126. This model relies on the fact that removal of the C-terminus electric charge by amidation led to a predominantly random-coil structure and inhibited fibril formation. These investigators suggested that the peptide molecules assemble in an antiparallel β-pleated sheet structure, which is stabilized by electrostatic interactions between positive charged residues of Lys^{106} and Lys^{110} and the negative charged carboxy group at the C-terminus. This model explains how elimination of the charge at the C-terminus shifts the equilibrium toward the random-coil monomeric state. However, as the authors conceded, this model cannot explain some of the experimental data: (1) the model cannot answer how an amidated peptide is still able to form a limited number of fibrils; (2) it does not express the important role of the His^{111} in the formation of the β-sheet structure; and (3) it can only explain the formation of dimer, but not of larger aggregates.

In this study, we focus on the first step of amyloid formation, which is the formation of intermediate PrP106–126 monomeric conformations. In particular, we aim to obtain an atomic level insight into the mechanism of the spontaneous transition of the PrP106–126 peptide from α-helical to β-sheet conformations and the interactions that stabilized the final state. Four 1–2-ns explicit solvent MD simulations and 30 implicit solvent MD simulations (10-ns each) of a solvated PrP106–126 peptide were carried out in this study, totaling 305 ns of simulation time (Table I). The dynamic properties of the wild-type peptide at neutral pH were investigated through two explicit solvent MD simulations, each starting from a different initial secondary structure conformation of the H1 region (residues 109–122). In one simulation, the initial conformation of the 14 H1 residues was an ideal α-helix, while in the other simulation the initial conformation of the same residues was the β-sheet conformation determined by x-ray studies of Inouye and Kirschner.[17] In both cases, the remaining residues on both sides of the H1 region (residues 106–108 and 123–126) were initially in an extended conformation. A comparison of the dynamics of the peptide starting from two different conformations may elucidate their relative stability, the interactions that govern the peptide's dynamics, and whether the two trajectories end up in similar conformations. To obtain better statistics on the dynamics and on the stability of the wild-type peptide, a set of an additional 10 trajectories, all starting from the

TABLE I. Summary of the Simulations Reported in This Study of the PrP106–126 Peptide

Simulation no.	Peptide	Initial conformation	Solvent model	pH	Length (ns)
1	Wild type	α-Helix	Explicit	Neutral	2
2	Wild type	β-Sheet	Explicit	Neutral	1
3	A117V mutant	α-Helix	Explicit	Neutral	1
4	Wild-type	β-Sheet	Explicit	Acidic	1
5–14	Wild-type	α-Helix	Implicit	Neutral	10
15–24	A117V mutant	α-Helix	Implicit	Neutral	10
25–34	Wild-type	β-Sheet	Implicit	Acidic	10

α-helical conformation, were simulated using an implicit solvent model.

The remaining MD simulations were performed in order to study the effects of an acidic pH and of the known A117V point mutation on the dynamic properties of the PrP106–126 fragment. The acidic pH environment may be introduced by the protonation of residues with pK_a values of <6. In the case of PrP106–126, this includes only His^{111}, which is protonated under these conditions and consequently becomes positively charged. As the goal was to explore stabilization of the β-sheet state at acidic pH, the acidic pH simulations started with the above β-sheet conformation. These include one explicit solvent MD simulation and 10 implicit solvent MD simulations. The initial conformation used in the simulation of the A117V mutated peptide was an α-helical structure, as in this case the goal was to see whether the mutation does, in fact, strengthen the hydrophobic interaction, leading to an early breakup of the α-helix. As in the previous case the dynamics of the A117V mutation was explored by one explicit solvent MD simulation and by an additional set of 10 trajectories, using an implicit solvent model.

METHODS

Explicit Solvent Simulations

Four explicit solvent MD simulations of the PrP106–126 peptide were carried out (Table I). In two of the simulations (1 and 3 in Table I), the initial conformation of the 14 residues in the H1 region (residues 109–122) was that of an ideal α-helix. In the other two simulations (2 and 4 in Table I), the initial conformation of these residues was the β-hairpin conformation determined in the x-ray study for the H1 fragment.[17] The Protein Data Bank (PDB) coordinates file of the H1 β-hairpin conformation was downloaded from http://www.mad-cow.org/~tom/prion_QuatStruc.html. The remaining residues on both sides of the H1 region were assigned an extended conformation. All peptides were with uncharged terminus, i.e., amine group (NH_2) at the N-terminus and carboxy group (COOH) at the C-terminus.

All simulations were performed using the CHARMM molecular dynamics program (version 26)[25] and the CHARMM all-atom force field.[26] The simulations used 1-fs time steps, the SHAKE constraints on bonds to hydrogen atoms, a dielectric constant of $e = 1$, and a 16-Å energy cutoff. The peptides were embedded in a 25-Å sphere of TIP3 water molecules, using stochastic boundary conditions. The water sphere was added in two steps, each of which involved overlaying a sphere of equilibrated water molecules at a random orientation followed by 20 ps of equilibration at 300 K. In the simulation that began with the α-helical structure, for example, 2,005 water molecules were added to the model in the first step, and 9 water molecules were added in the second step, for a total of 2,014 water molecules. The total number of atoms in this simulation (peptide and water) was 6,314.

Implicit Solvent Simulations

The size of the system makes it difficult to obtain statistical samples of the dynamic and thermodynamic behavior of the peptide, using the explicit water simulations. To overcome this limitation, this study uses the EEF1 implicit solvent model,[27] which expresses the solvation free energy as a sum over group contributions, with the solvation free energy of each group corrected for the screening by surrounding groups. The EEF1 has been shown to give reasonable energies for unfolded and misfolded conformations[27] and unfolding pathways, in agreement with explicit water simulations.[28] To obtain statistical data for the α-helix unwinding and for the interaction stabilized the coil structures of both wild-type and A117V PrP106–126, 10 trajectories (10-ns each) were simulated for each sequence (Table I). An additional set of 10 trajectories (10-ns each) were simulated for the wild-type PrP106–126 at acidic pH (simulations 25–34 in Table I). The trajectories differ one from the other by the value of the seed used for generation the random numbers that assign the initial velocities.

Simulation Protocol

In all the simulations, the initial solvated PrP106–126 peptides were gradually heated to 300 K for 10 ps of dynamics. The system were then simulated for 1 ns (except the simulation 1 began with an α-helical conformation at neutral pH, which was simulated for 2 ns) at 300 K, from which conformations were sampled every 0.2 ps. A total of 4,000 conformations (8,000 for the 2-ns trajectory) were collected from the MD trajectories of each system. The inter-residue distances are calculated between the C_β of alanine, the C_ϵ of methionine, the center of mass of C_β, and the two C_γ atoms of valine, as well as the center of mass of the imidazole ring of histidine. The α-helix and β-sheet content of each conformation throughout the four trajectories were calculated using the DSSP program.[29]

Projection of the trajectories onto subspace of the conformation space was obtained by applying the principal component analysis (PCA) method.[30,31] The PCA projects multidimensional data onto low-dimensional subspaces by selecting a new set of principal axes that best preserve the distances between the conformations, enabling visualization of the spatial relations between the data points. The PCA is a very useful method with which to visualize significant conformational changes such those expected for PrP106–126; it may reflect the effects of acidic pH and of the A117V point mutation on the structural transition. For the present application, it should be noted that when conformations of two analogous molecules are to be compared, they must be projected together onto the same subspace. As a consequence, the distance measure used should be based on features common to the two molecules. In this study, we use the root-mean-square deviation (RMSD) of the backbone heavy atoms as the distance measure between conformations of different trajectories. The principal two-dimensional (2D) subspace represents the multidimensional data to accuracy of greater than 50%.

RESULTS AND DISCUSSION

The PrP106–126 Helix-Coil Conversion

CD and NMR studies have shown that the α-helical conformer of PrP106–126 is stable in organic solvents but tends to convert to a β-strand structure in water, eventually leading to fibril formation.[22,23] To assess the stability of the α-helical state of the wild-type PrP106–126 in water and to characterize its conversion to the β-strand state, a 2-ns simulation of the 21-amino acid peptide with explicit water molecules was performed, starting with a conformation in which residues 109–122 (H1 fragment) form an ideal α-helix (i.e., 66% α-helical content for the whole peptide) that has been pre-equilibrated.

The changes in the percentage of helicity of the wild-type peptide along the 2-ns explicit solvent MD simulation are shown in Figure 1. The α-helical content of PrP106–126 at the beginning of the simulation is about 66%. The helical content begins to decrease after 0.5 ns, reaching about 20% after 0.7 ns and rebounding to 50%; finally, the peptide completely loses its α-helix characteristic (0% α-helix) after 1.5 ns. This observation indicates that the conversion of PrP106–126 from an α-helix to a random coil structure is very efficient. Because simulating the system with an explicit solvent model is very time-consuming, a set of 10 MD simulations (10-ns each) that use the EEF1 implicit solvent model[27] were performed to add statistical significance to the interpretation of the α-helix breakup and the stabilizing interactions of the coil structures (simulations 5–14 in Table I). Figure 2 shows the distribution of the times required for the breakup of the helix in wild-type PrP106–126 based on the 10 implicit solvent simulations (simulations 5–14 in Table I). This distribution indicates that the average time for the helix breaking is 4.3 ns. This time is longer than the time obtained from the explicit solvent calculations (1.5 ns); the difference should be attributed to the different screening of interactions by the explicit and implicit solvation models. However, it should be noted that to study the effect of the A117V mutation, it is the relative, and not the absolute, time scale that is important.

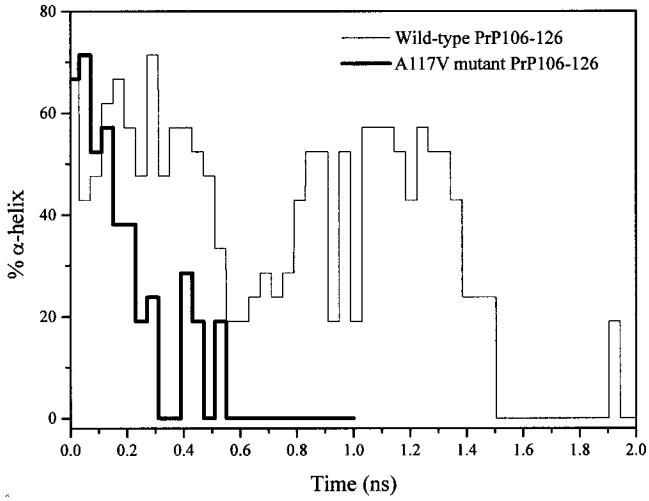

Fig. 1. α-Helical content of PrP106–126 along the 2-ns explicit solvent trajectory of wild-type PrP106–126 (simulation 1) and along the 1-ns explicit solvent trajectory of the A117V mutant (simulation 2). Both simulations were performed with explicit water molecules at neutral pH. The initial α-helix content of PrP106–126 is about 66%. It is seen that introducing the A117V mutation reduced the time it took the peptide to convert from an α-helical to a random-coil structure by 1 ns. The α-helical percentage was calculated using the DSSP program.

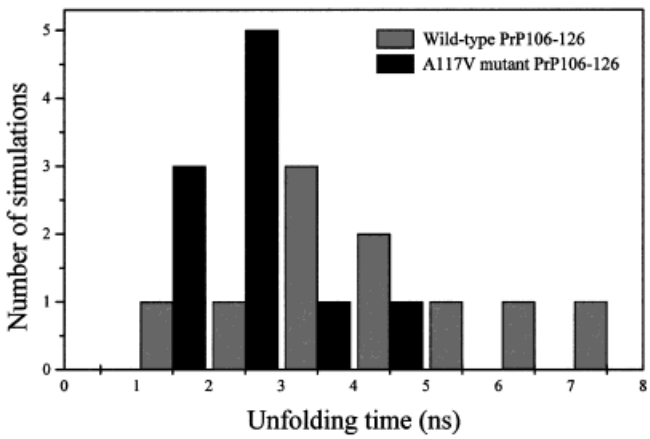

Fig. 2. Distribution of the times required for helix breakup in both wild-type and A117V mutant PrP106–126. Each distribution is based on 10 implicit solvent simulations (simulations 5–14 for the wild-type and simulations 15–24 for the A117V mutant PrP106–126). A comparison between the two distributions indicates that helix breaking for the mutant peptide is faster by 1 ns than for the wild-type in agreement with the explicit solvent simulations.

To identify the pattern in which the helix break, the 9 hydrogen–bond distances [NH(i)–CO(i+4)] that define the α-helix between residues 109–121 were followed throughout the simulation (Fig. 3). During the first 0.5 ns, all hydrogen bonds are intact. However, starting at 0.5 ns, the hydrogen–bond distances between NH^{112}–CO^{116} and NH^{113}–CO^{117} begin to increase, reaching 7Å at 0.7 ns, indicating that these two hydrogen bonds no longer exist;

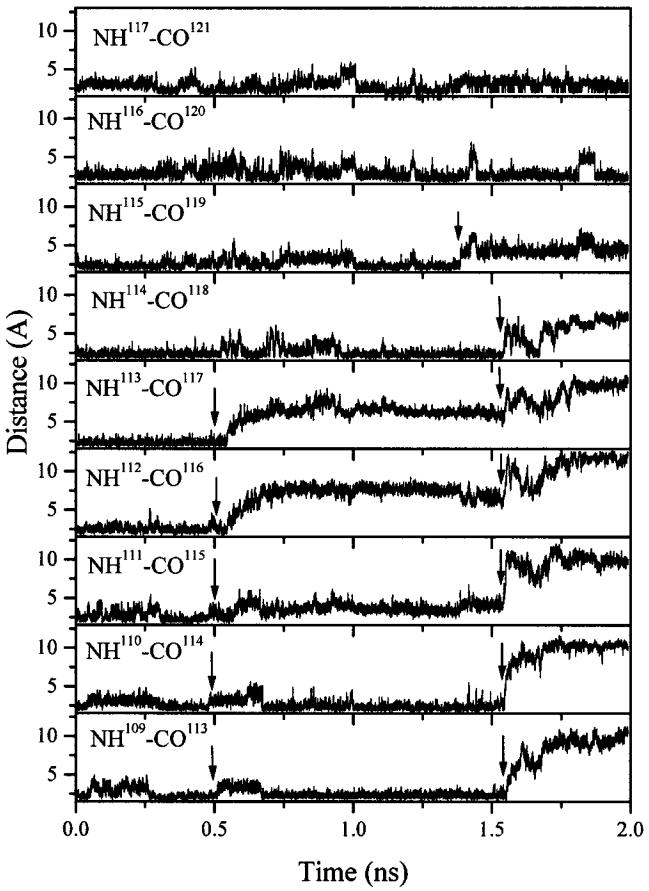

Fig. 3. Nine hydrogen–bond distances that define the H1 α-helix during the explicit solvent simulation of wild-type PrP106–126 that started with an α-helical conformation (simulation 1 in Table I). The distances are between NH(*i*) and CO(*i*+4), where *i* ranges from residue 109 to residue 117. Arrow indicates when the hydrogen bonds break. The observed pattern indicates that the wild-type helical PrP106–126 begins to break up in the middle, forming two smaller helices, and is followed by unwinding of the N-terminus fragment.

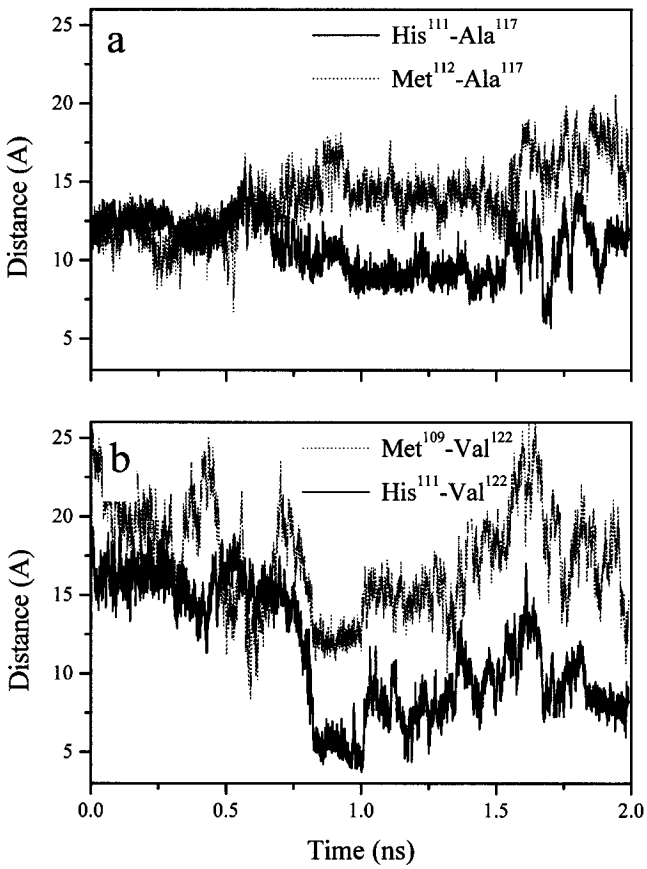

Fig. 4. Four PrP106–126 intramolecular distances along the explicit solvent trajectory 1. **a:** The distances between His^{111} and Ala^{117} and the distance between Met^{112} and Ala^{117}. During the simulation these distances do not significantly decrease below the initial values of 12 Å, indicating that Ala^{117} does not interact with either His^{111} or Met^{112}. **b:** The distances between Met^{109} and Val^{122} and the distance between His^{111} and Val^{122}. During the simulation, the His^{111}–Val^{122} distance decreases from 17 Å to 4 Å at the same time, when the α-helix content of the peptide start to decrease.

that is, the α-helix begins to break at the middle of the peptide, between residues 112–117. Significant fluctuations in the distances of the other hydrogen bonds are also observed between 0.5–0.7 ns. These strong fluctuations are responsible for the temporary decrease of the α-helix content after 0.7 ns (Fig. 1). After an additional 1 ns of simulation, four more hydrogen bonds start to break (NH^{109}–CO^{113}, NH^{110}–CO^{114}, NH^{111}-CO^{115}, and NH^{114}–CO^{118}). This is accompanied by a further increase in the distance between the components of the two broken hydrogen bonds (NH^{112}–CO^{116}, NH^{113}–CO^{117}). At the end of the simulation, after 2 ns, only two of the original α-helix hydrogen bonds located, at the C-terminus region of the peptide, remained although even these two become weaker. This very short and unstable α-helical region corresponds to the 0–18% α-helical content after 1.5 ns, as shown in Figure 1.

The breakup of the α-helix in the middle creating two smaller helices, which is followed by unwinding of the C-terminus fragment, can be viewed as the first step toward the formation of a β-hairpin stabilized by hydrophobic interactions. As discussed above, it was previously suggested that the β-sheet conformation of the 14 residues H1 fragment is stabilized by a hydrophobic interaction between residues His^{111}–Ala^{117}. If this suggestion is correct, it should hold true also for the larger PrP106–126 peptide.

To see whether such stabilizing interactions are formed after the breakup of the original α-helix, we followed four distances between different hydrophobic residues, one on each of the two strands that might contribute hydrophobic interactions (Fig. 4). These residues are His^{111} and Met^{112} on one strand and residues Ala^{117} and Val^{122} on the other strand. Figure 4(a) demonstrates that the distances between His^{111} and Ala^{117} and between Met^{112} to Ala^{117} are beyond the range of any significant interaction throughout the simulation. Similar results were obtained in the 10 simulations (10-ns each) that use the EEF1 implicit solvent model. Figure 4(b) depicts the distances between Met^{109} and Val^{122} and between His^{111} and Val^{122}. Initially, when the peptide is predominantly in its α-helical conformation, both distances are too large for the residues

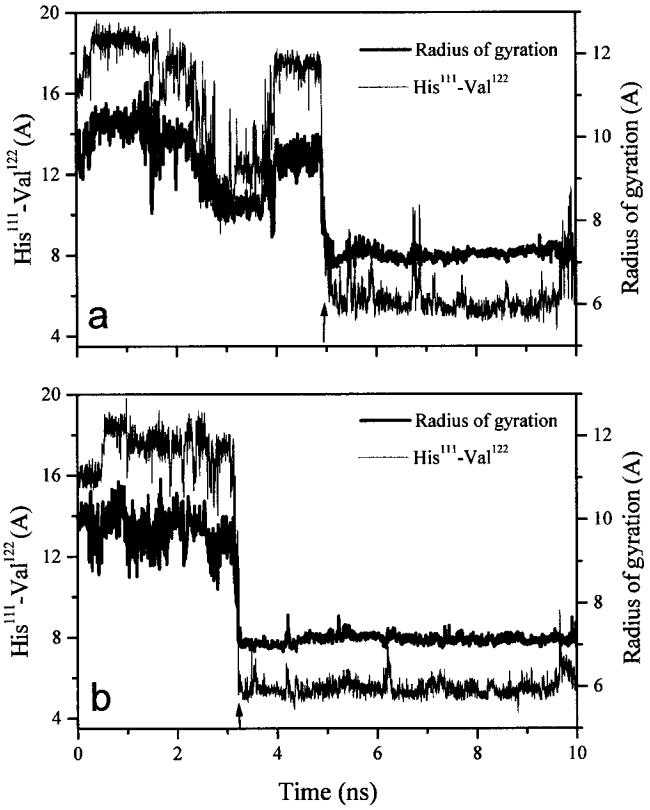

Fig. 5. His^{111}–Val^{122} distance and the radius of gyration along two of the 10 implicit solvent simulations of wild-type PrP106–126 (6 in **a** and 8 in **b**). The structural transition (indicated by arrows) occurs 5 ns and 3.2 ns after the beginning of the simulations, respectively.

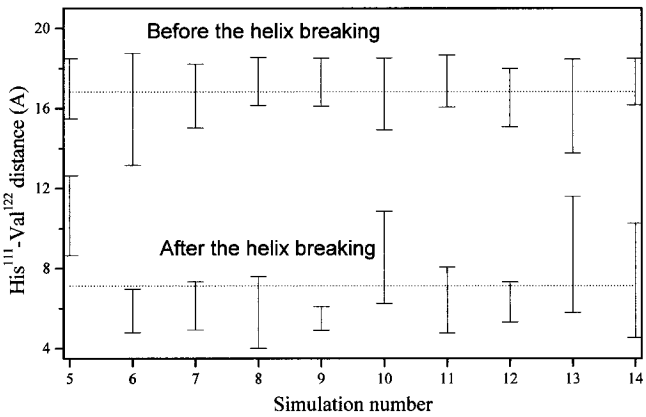

Fig. 6. Average His^{111}–Val^{122} distance and its standard deviation before and after helix breakup in each of the 10 implicit solvent trajectories of wild-type PrP106–126 (simulations 5–14 in Table I). His^{111}–Val^{122} distance averaged over the set of 10 trajectories, before and after helix breakup, is 16.8 Å and 7.1 Å, respectively.

to interact. However, while the distance Met^{109}–Val^{122} remains large throughout the 2-ns simulation, the His^{111}–Val^{122} distance decreases significantly from 18 Å to 4 Å, indicating the presence of hydrophobic interaction. The decrease in the His^{111}–Val^{122} distance begins after 0.5 ns, the same time at which the helix starts to break up, reaching a minimal value at 1.0 ns. To demonstrate the peptide structural transition in the implicit solvent model, the His^{111}–Val^{122} distance, together with the radius of gyration, along two of the implicit solvent simulations (simulations 6 and 8) are presented in Figure 5. In both simulations, the structural transition is reflected by a sudden decrease of the radius of gyration and is associated with a significant decrease in the His^{111}–Val^{122} distance. In these two simulations (6 and 8), the decrease in the His^{111}–Val^{122} distance occurs at 5 ns and 3.2 ns after the beginning of the simulation, respectively, and indicates a formation of hydrophobic interaction that remains stable until the end of the simulations. The average His^{111}–Val^{122} distance in each of the 10 implicit solvent trajectories (simulations 5–14) both before and after the helix breaking is shown in Figure 6. The average His^{111}–Val^{122} distance in the helical structure, averaged over the 10 implicit solvent simulations, is 16.8 Å. However, this average decreases to 7.1 Å after the helix breaks up, indicating the importance of this interaction in the stabilization of the resulting β-hairpin structures.

The hydrophobic interactions between His^{111} and Val^{122} are in agreement with several experimental studies.[17,22] However, the simulation indicates that this stabilization occurs not through interaction with Ala^{117}, as suggested by the crystallographic structure of the β-sheet conformation of the H1 peptide,[17] but rather through interaction with Val^{122} (the interaction His^{111}–Val^{121} also contributes to the hydrophobic interaction between the two strands). After 1 ns of the explicit solvent simulation, the His^{111}–Val^{122} distance starts to increase again, although it remains fairly short for the remainder of the simulation. The resulting His^{111}–Val^{122} distances in the explicit solvent simulation, as well as in the 10 implicit solvent simulations, indicate that this His–Val interaction plays an important role in destabilization of the α-helical structure and in stabilization of the monomeric β-hairpin structure. However, in several of the implicit solvent trajectories (e.g., 5, 10, and 13; see Fig. 6), stabilization of the monomeric β-hairpin structure by this interaction was weaker, and in these simulations the peptide also adopted a coil structure. It is possible that upon aggregation, the interaction between His^{111} and Val^{122} will continue to contribute to the stabilization of the monomeric β-hairpin structure.

To assess further the role of the His^{111}–Val^{122} interaction, as compared with that of the His^{111}–Ala^{117} interaction, in stabilizing the β-sheet conformation of the PrP106–126 peptide, a 1-ns explicit solvent MD simulation was carried out. This simulation (2 in Table I) was carried out under the same conditions and in the same chemical environment as the previous explicit solvent simulation; the only difference was the initial structure, which in this case was based on the crystallography determined β-sheet structure of the 14-residue H1 fragment. Recall that this structure is characterized by a His^{111}–Ala^{117} hydrophobic interaction.[17] It was found in agreement with the results of simulation 1, that the distance between His^{111} to Ala^{117} gradually actually increased from 4 Å to 16 Å over the 1-ns course of the simulation. This increase enabled the forma-

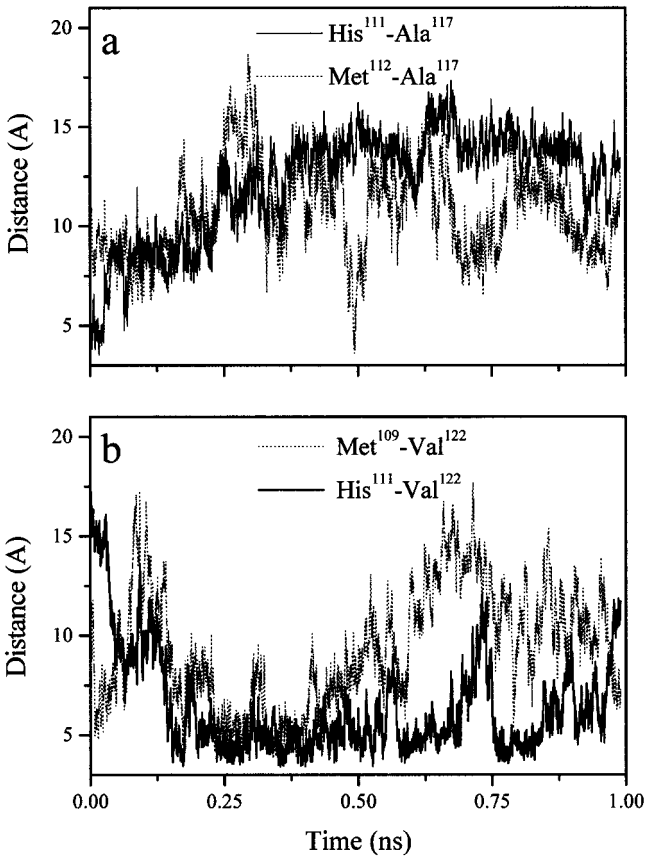

Fig. 7. Same as Fig. 4, but for explicit solvent trajectory 2 that starts from a β-structure. The distance between His^{111} to Ala^{117}, which is 4 Å in the initial β-sheet structure increases to 16 Å, while a more favorable hydrophobic interaction between His^{111} and Val^{122} is being formed.

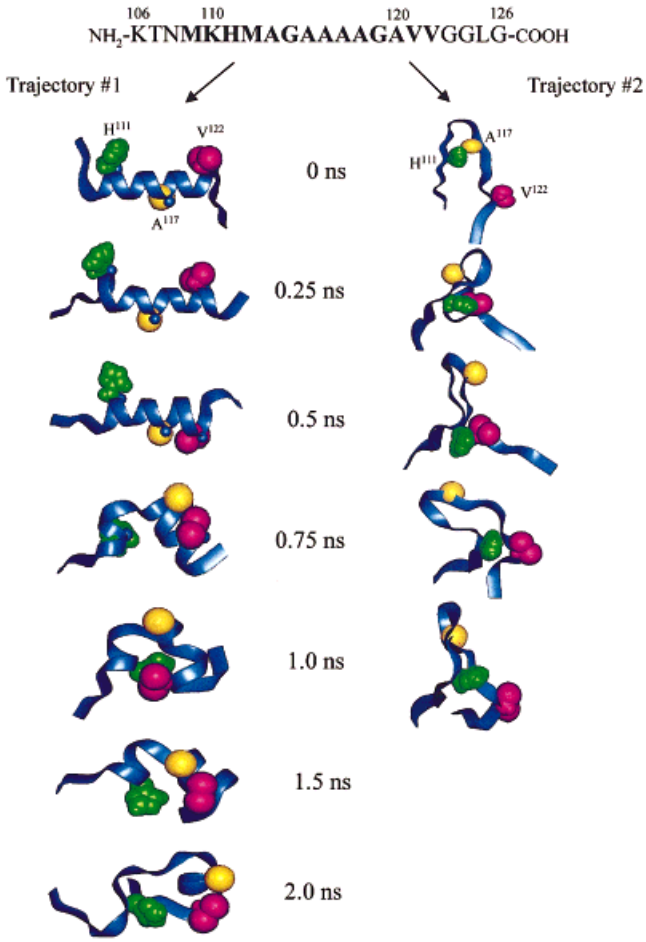

Fig. 8. Twelve snapshots of PrP106–126 extracted from the explicit solvent simulations 1 and 2 are shown. The seven snapshots on the right are from simulation 1 that started from an α-helical conformation; the five structures on the left are from simulation 2 that started from a β-sheet conformation (all structures were taken at 0.25-ns interval). The side-chains of His^{111}, Ala^{117}, and Val^{122} are represented by green, yellow, and pink vdW spheres, respectively, and the backbone by a ribbon. The seven structures of simulation 1 illustrate how the conformation changes during the dynamics from a predominantly α-helical to a random-coil structure. The five structures of simulation 2 illustrate that the overall β-sheet secondary structure of the PrP106–126 remains during this simulation. The role of the His^{111}–Val^{122} interaction is illustrated in both sets of structures.

tion of the more favorable hydrophobic interaction between His^{111} and the valine residues (121 and 122). Figure 7 demonstrates the increase in the His^{111}–Ala^{117} distance [Fig. 7(a)] and the decrease in the His^{111}–Val^{122} distance [Fig. 7(b)]. Figure 7 suggests that Met^{109} also contribute to the stabilized hydrophobic core that is formed, although its contribution is smaller than that of His^{111}.

Figure 8 exhibits several snapshots of the PrP106–126 peptide, which were extracted from two MD trajectories. Seven structures were taken from the 2-ns simulation (simulation 1 in Table I) that started with an α-helical conformation; five structures were taken from the 1-ns simulation (simulation 2 in Table I) that started with β-sheet conformation. The snapshots originating from the trajectory that started with an α-helical conformation illustrate how the peptide converts from a predominantly α-helical conformation to a random coil conformation, in which a hydrophobic interaction between the histidine residue and the valine residue is being formed. The helix breakup initiates near residues Ala^{114} and Ala^{115} and it is assisted by the hydrophobic interaction between residues His^{111} and Val^{122}. These snapshots also indicate that after the helix is broken, this hydrophobic interaction becomes weaker and the peptide ends up in a random coil conformation. Clearly, 2 ns was not enough time to get the α-helical structure into a β-sheet conformation. Evidently, longer simulations in explicit water are required in order to observe an α→β transition. The five snapshots from the second simulation that started from the β-sheet conformation illustrate that the overall β-sheet secondary structure of PrP106–126 is retained during the 1-ns simulation, with the exception that the histidine residue forms a hydrophobic interaction with Val^{122}, and not with Ala^{117}.

Figure 8 also shows that the above two simulations, each starting from a different initial structure, did not converge into the same final conformation. To highlight the conformational relationship between the two simulations, the two dynamic trajectories were jointly projected onto the same principal 2D plane by applying the principal component analysis (PCA) method.[30,31] The resulting principal

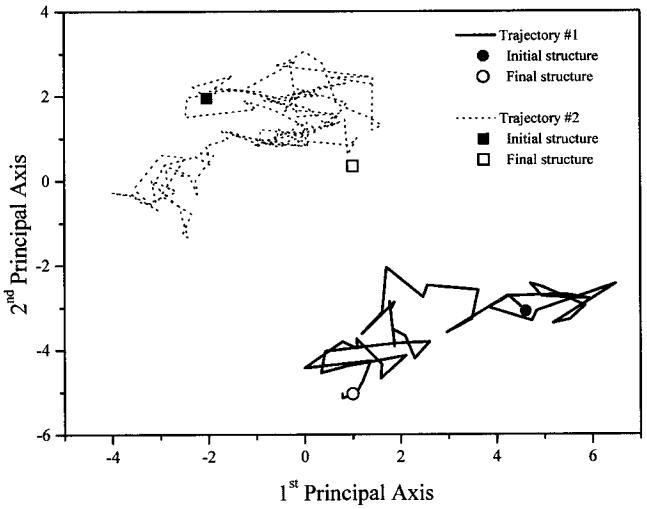

Fig. 9. Joint 2D projection of the two explicit solvent trajectories of the wild-type peptide starting from the α-helical and β-sheet conformations (simulations 1 and 2). Trajectory is projected on the first two principal axis obtained by applying the principal component analysis method. The projection shows that the initial conformations are located very far from each other in two different regions of the conformation space of the peptide. However, as the dynamics progresses, conformations sampled by the two trajectories become closer to each other, indicating more similar structures.

coordinate projection (Fig. 9) shows that the two initial conformations, the α-helix and the β-sheet, are indeed located very far from each other in two different regions of the peptide's conformation space. However, as the dynamics progresses the conformations sampled by the two trajectories become closer to each other in this projection, indicating increasing similarity between the structures. While the backbone RMSD between the two initial conformations (the α-helical and the β-sheet conformations) is 9.24 Å the two trajectories generate structures as close as 4.06 Å to one another (although the distance between the two final conformations is larger). Thus, the PCA projection of the trajectories indicates that while the simulations had started from very different structures the dynamics brings them closer together. It is reasonable to assume that simulating the system for even longer periods of time will result in convergence of the final structures.

Effect of A117V Mutation on the Stability of PrP106–126

Substitution of alanine by valine at position 117 is linked to the GSS disease (as was mentioned above),[2] possibly by favoring the random-coil state over the α-helical one. A crystallographic study conducted by Inouye and Kirschner[17] showed that His^{111} faces Ala^{117} in the β-sheet conformation of the H1 region. Therefore, these researchers suggested that a replacement of Ala by Val may facilitate the formation of a H1 β-sheet due to the stronger hydrophobic interactions between His and Val. A MD study of the H1 peptide conducted by Kazmirski et al.,[24] which explored alternative replacements of Ala^{117} with hydrophobic amino acid residues showed that only the substitution of Val^{117} for Ala^{117} had a destabilizing effect on the helix.

To study the stability of the α-helix conformation for the A117V mutant PrP106–126 peptide, a MD simulation was performed with explicit water molecules (simulation 3 in Table I). This 1-ns simulation of the solvated mutant peptide started from a conformation in which residues 109–122 (the H1 fragment) adopt an α-helix structure. The percentage of α-helix throughout this 1-ns simulation is shown in Figure 1. As can be seen, the mutant peptide loses its α-helix character much faster than does the wild-type. The α-helical content of the mutant peptide begins to decrease as early as 0.1 ns after the beginning of the simulation and the peptide becomes completely nonhelical (0% α-helix) after 0.5 ns of simulation. This time scale is significantly shorter than the time scales associated with the loss of helicity in the wilde-type peptide, on the order of 1.5 ns. To obtain better statistics for this helix breakup event, an additional set of 10 implicit solvent trajectories (10-ns each) (simulations 15–24 in Table I) of the A117V mutant PrP106–126 were simulated. The distribution of the times it took the α-helical conformation in the A117V mutant peptide to break up, based on these 10 implicit solvent simulations is shown in Figure 2. The average time for helix breakup is 2.8 ns. A comparison between this distribution for the mutant and for the wild-type PrP106–126 in implicit solvent agrees with the calculations derived from the explicit solvent simulations (Fig. 1). Namely, for the A117V mutant, the helix breakup process is shorter by 1 ns, as compared with the equivalent process for the wild-type. The simulations show that introducing the A117V mutation substantially destabilizes the α-helix, accelerating its dissociation, and reducing the total time for losing all α-helical features by approximately 1 ns.

Following the nine hydrogen–bond distances that define the H1 α-helix (residues 109–121) during the 1-ns explicit solvent simulation of the A117V mutant shows that the helix breakup pattern in the mutant is different from that of the wild-type (Fig. 10). In the mutant, the first hydrogen bonds to break are those located at the C-terminus region of the peptide. These hydrogen bonds are lost as early as 0.1 ns after the beginning of the simulation. Later, the hydrogen bonds at the middle of the helix, and then at the N-terminus region, break up; by $t = 0.8$ ns, no remnant of the α-helix defining hydrogen bonds remains. Namely, the mutated peptide starts to break at the C-terminus region, followed by a gradual unwinding of the helix that ends after 0.8 ns with disruption of the hydrogen bonds in the N-terminus region of the peptide. This mechanism is different from the mechanism that was observed for the wild-type PrP106–126, in which the α-helix break up initiates in the middle of the peptide and then continues to the N-terminus.

To determine what hydrophobic interactions contribute to the observed dynamics of the mutant peptide, we calculated for the explicit solvent simulation the same four inter-residue distances that were calculated for the wild-type peptide (Fig. 4). Figure 11(a) shows that in the initial ideal α-helical conformation, both the His^{111}–Val^{117} and the Met^{112}–Val^{117} distances are about 12 Å. However,

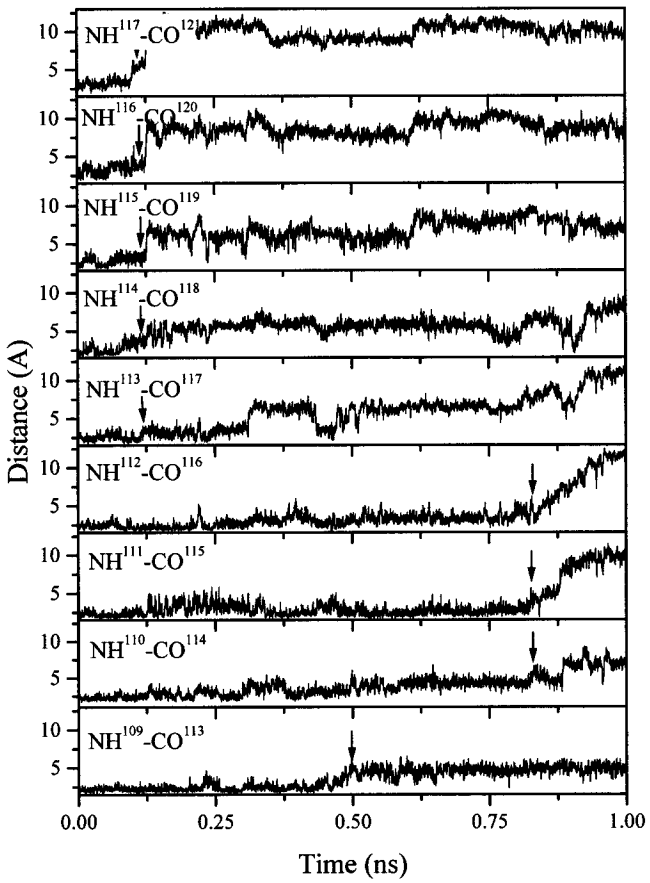

Fig. 10. Same as Fig. 3, for explicit solvent simulation of the A117V mutant (simulation 3), starting with an α-helical conformation. The first hydrogen bonds to break up are those at the C-terminus region of the peptide and occur after 0.1 ns. Later, the other hydrogen bonds at the middle and at the N-terminus region start to break up, and no hydrogen bonds that define an α-helix can be found after 0.8 ns.

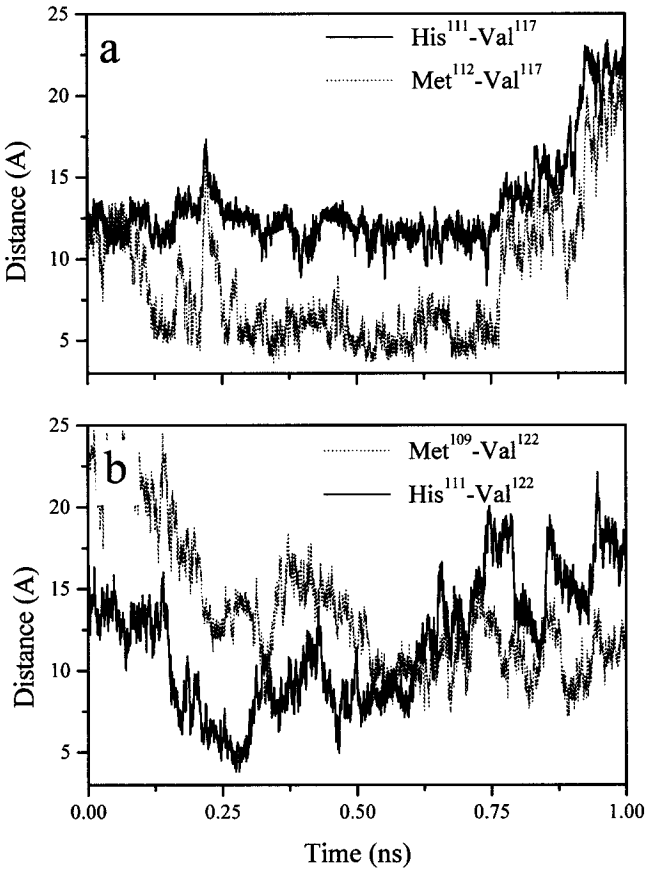

Fig. 11. Same as Fig. 4, but for simulation 3. These distances indicate that the interactions between Met^{112} and Val^{117} and between His^{111} and Val^{122} govern the breakup of the α-helix of A117V mutant. Met^{112}–Val^{117} interaction is unique to the A117V mutant.

although the His^{111}–Val^{117} distance does not decrease during the 1-ns simulation, the Met^{112}–Val^{117} distance decrease after <0.1 ns, to a value of about 5 Å, indicating a strong hydrophobic interaction that persists for almost 0.7 ns [Fig. 11(a)]. The formation of the Met^{112}–Val^{117} hydrophobic interaction was also observed in 7 of the 10 implicit solvent simulations of the A117V mutant (simulations 15–24 in Table I). In three of these seven simulations, the interaction was strong and persisted from the point of helix breaking to the end of the simulation. In the other four simulations, the interaction was less stable and existed only for 1–2 ns. The Met^{112}–Val^{117} distance along two such implicit solvent simulations (simulations 22 and 23 in Table I) is depicted in Figure 12, together with the radius of gyration. These simulations illustrate the existence of Met^{112}–Val^{117} interactions for short (1.5-ns) and long (≥7-ns) periods, respectively. It should be stressed that this interaction, which is dominant during the breaking of the α-helix of the mutant peptide, is not formed in the wild-type peptide, which has an alanine at position 117 [Fig. 4(a)]. The Met^{109}–Val^{122} and His^{111}–Val^{122} distances from the explicit solvent simulation are shown in Figure 11(b). These distances, which are about 23 Å and 16 Å, respectively, in the α-helix structure, begin to decrease within the first 0.2 ns, although only His^{111}–Val^{122} form a stabilizing interaction for a short period of time. In the implicit solvent simulations of the A117V mutant, the His^{111}–Val^{122} interaction was found only in 3 of the 10 trajectories, while in the other 7 trajectories (in which the Met^{112}–Val^{117} hydrophobic interaction is dominant), no evidence to the His^{111}–Val^{122} interaction was found. This behavior is different from that of the wild-type peptide [Figs. 4(b), 6]; that is, while the wild-type peptide forms a His^{111}–Val^{122} hydrophobic interaction during the α-helix breakup, the A117V mutant peptide forms a hydrophobic interaction between Met^{112}–Val^{117}. The different stabilizing interactions, His^{111}–Val^{122} in the wild-type versus Met^{112}–Val^{117} in the mutant, lead to the different mechanisms of the helix breaking that were observed. While in the wild-type peptide the His^{111}–Val^{122} interaction causes the helix to break up into two fragments, the substitution of Ala by Val at position 117 leads to a hydrophobic interaction with Met^{112} that results in an unwinding of the C-terminal of the peptide.

Figure 13 exhibits five snapshots that were extracted from the explicit solvent simulation of the A117V mutant at 0.25-ns intervals. A comparison between these snapshots with those obtained from the wild-type simulation

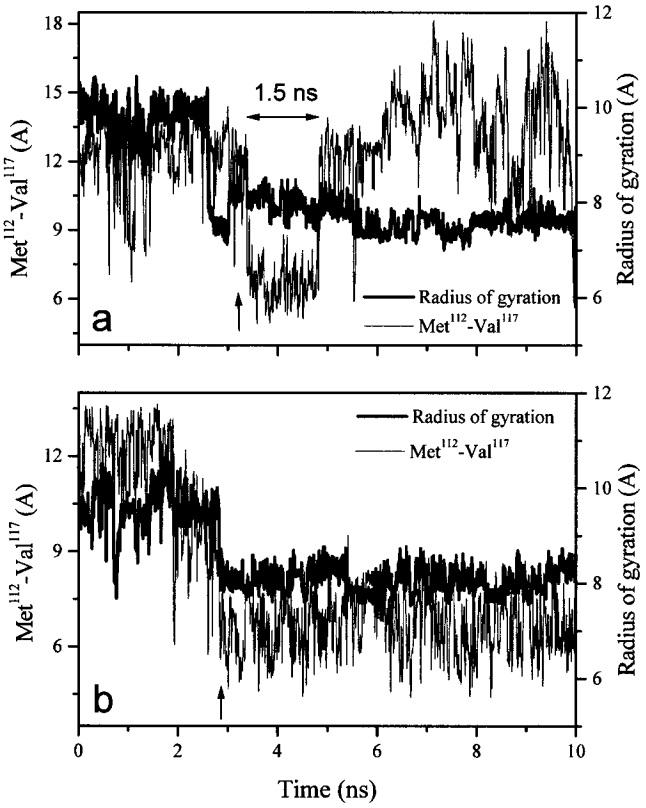

Fig. 12. Met^{112}–Val^{117} distance and the radius of gyration along two of the 10 implicit solvent simulations of A117V mutant PrP106–126. The structural transitions in these simulations (simulation 22 in **a** and 23 in **b**) occur 3.2 ns and 3.0 ns after the beginning of the simulations (indicated by arrows). While in simulation 22 (a) the Met^{112}–Val^{117} hydrophobic interaction exists only for 1.5 ns, its stability is greater in simulation 23 (b).

(Fig. 8) illustrates how the A117V mutation accelerates the helix breaking process, affecting both its mechanism and its time scales. The simulation also shows that the role of the hydrophobic interactions in both wild-type and mutant is to stabilize the two halves of the peptide during the helix breaking phase. However, once the helix has dissociated, these interactions become less dominant.

Because the normal and mutated PrP106–126 exhibit different dynamic behavior, we again apply the principal component analysis method to compare the two trajectories. A joint projection of the wild-type and A117V mutant explicit solvent trajectories, starting both from a similar α-helical conformation, onto the first two principal axes, is shown in Figure 14. Naturally, the two initial conformations appear very close to each other, as they are both α-helical structures (with RMSD of 0.89Å between them). However, the final structures for the two peptides are very different from one another (with RMSD of 9.95 Å). In fact, the distance between the two final structures is larger than the RMSD between the α-helical and β-sheet conformations of the wild-type peptides itself. The rather limited overlap between the two trajectories also supports the observation that starting from an initial α-helix structure the wild-type and mutant reach the final random-coil conformations along different pathway.

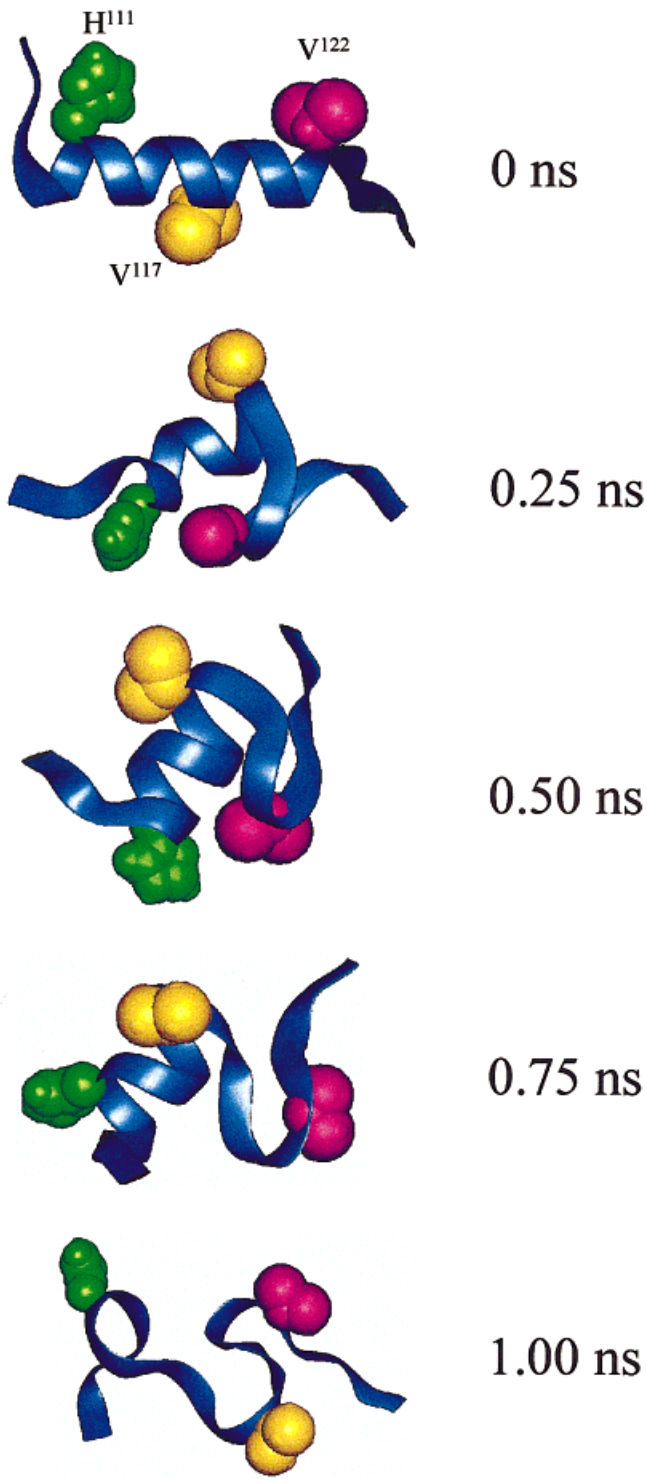

Fig. 13. Five snapshots of the A117V mutant extracted from the 1ns explicit solvent simulation (simulation 3 in Table I) at 0.25-ns intervals. The side-chains of residues His^{111}, Val^{117}, and Val^{122} are represented by green, yellow, and pink vdW spheres and the backbone by a ribbon. Comparison between these structures with those of the wild-type peptide (Fig. 8) illustrates that both the rate and the mechanism of helix break up are affected by the A117V mutation.

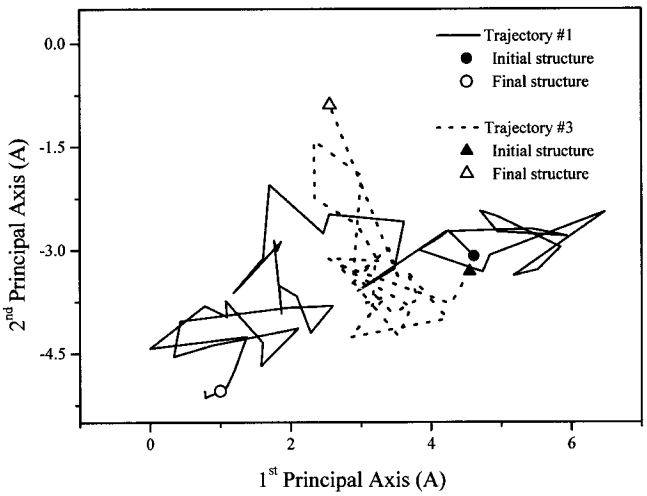

Fig. 14. Joint projection of the wild-type and A117V mutant explicit solvent trajectories (simulations 1 and 3). The two initial conformations appear very close to each other since both are α-helical structures (with RMSD of 0.89Å between them). However, the two final structures of the two peptides are very different from one another (with RMSD of 9.95 Å).

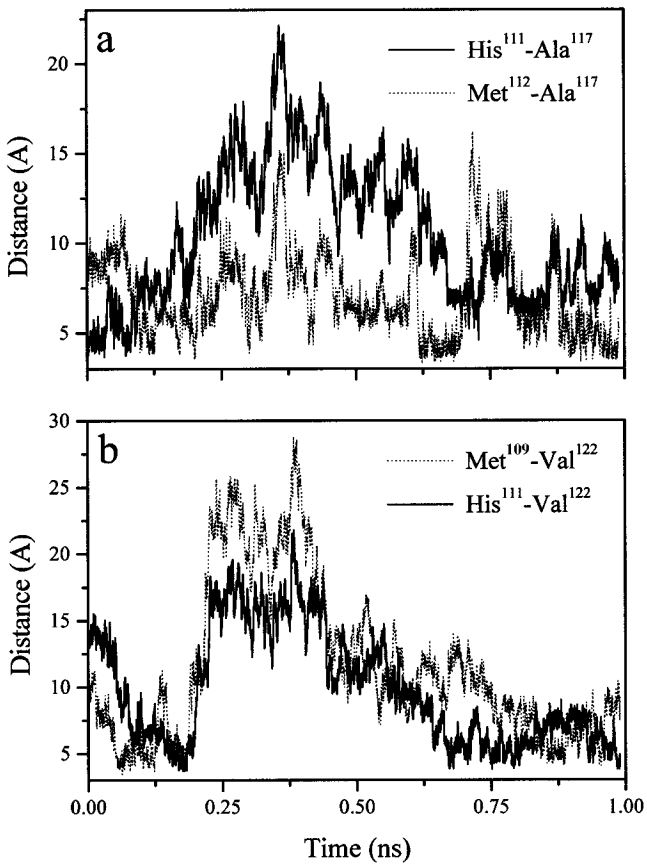

Fig. 15. Same as Fig. 3 for the explicit solvent simulation of wild-type PrP106–126 at acidic pH, starting with a β-sheet initial structure (simulation 4).

The Effect of Acidic pH on the Stability of Wild-Type PrP106–126

Based on a crystallographic study,[17] it was proposed that the H1 fragment of the prion protein adopts an extended conformation at acidic pH. At low pH values, the single histidine residue of the peptide is protonated positively and becomes charged. As a result, its side-chain no longer participates in the hydrophobic interaction that stabilizes the β-sheet conformation of the peptide. At higher pH values (>pH 5.2), the histidine is deprotonated and may contribute to the stability of the β-sheet.[19] Besides the effect of the pH value on the secondary structure content of the peptide, there is an additional pH effect on its aggregation properties. Salmona et al.[22] found that replacing His^{111} with a residue that is not sensitive to pH, such as alanine, did not affect aggregation upon reducing the pH value. This finding is in contrast to the reduced aggregation propensities at pH 5 for both wild-type and A117V mutant PrP106–126, despite the fact that both peptides have higher β-sheet contents at acidic pH. These researchers suggested that at acidic pH the peptide monomers are capable of adopting a β-sheet conformation, while at the same time the propensity of the peptides to aggregate was reduced by antagonizing the intramolecular hydrophobic forces.

To examine the propensity of a wild-type PrP106–126 monomer to maintain a β-sheet structure at acidic pH, we have carried out one 1-ns explicit solvent MD simulation (simulation 4) and 10 implicit solvent simulations (10-ns each) (simulations 25–34 in Table I). The acidic pH was introduced into the simulation by protonating His^{111}, which is the only residue in that peptide that changes its protonation state between pH 5.0 and 7.0. The terminal amine and carboxy groups were maintained uncharged in order to enable a comparison between this prion fragment and whole prion protein. The initial conformation was similar to the β-sheet structure used in simulation 2, a conformation that reflects a hydrophobic interaction between His^{111} and Ala^{117}.

As in the other three explicit solvent simulations, four inter-residue distances that may contribute hydrophobic interactions were followed during this 1-ns explicit solvent simulation of the wild-type peptide at acidic pH (simulation 4). The His^{111}–Ala^{117} and Met^{112}–Ala^{117} distances are shown in Figure 15(a) and the Met^{109}–Val^{122} and His^{111}–Val^{122} distances are shown in Figure 15(b). Because the starting structure is that of a β-sheet stabilized by a hydrophobic interaction between His^{111} and Ala^{117}, the initial distance between these two residues is short. As was observed in the equivalent simulation at neutral pH (Fig. 7), the His^{111}-Ala^{117} distance increases and the His^{111}–Val^{122} distance decreases as the simulation progresses, indicating an interaction between His and Val. However, the observed fluctuations in this distance indicates that the stability of this interaction at acidic pH is lower than that at neutral pH. Strong fluctuations are observed also for the other three distances reflecting larger degree of flexibility for the peptide at acidic pH. Thus, the destabilization of the interaction between His and Val at acidic pH results in increasing the peptide flexibility and thus its capability to adopt other partially stable conformations. To add statistical significance to the above dynamic

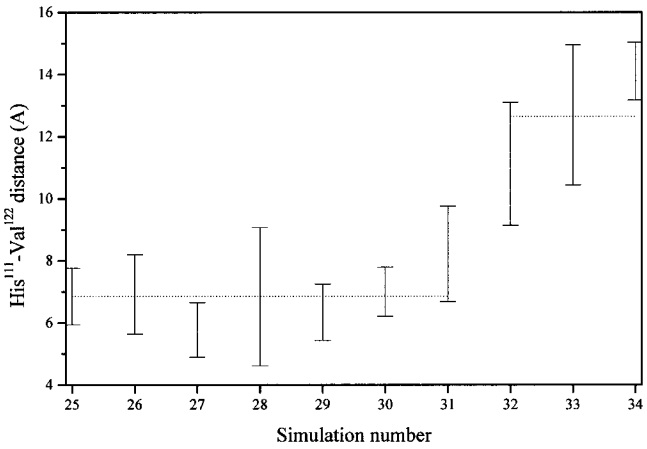

Fig. 16. Average His^{111}–Val^{122} distance and its standard deviation in each of the 10 implicit solvent trajectories of wild-type PrP106–126 at acidic pH (simulations 25–34 in Table I). In seven simulation, the average His^{111}–Val^{122} distance in 7 simulations is 6.8 Å, while in the other three simulations it is 12.6 Å.

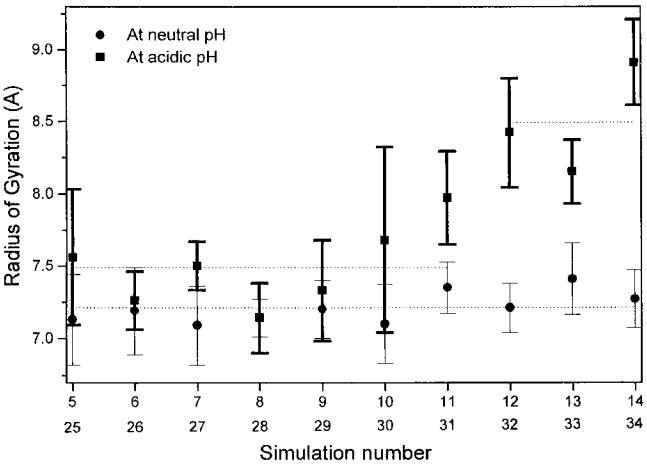

Fig. 17. Average radius of gyration and its standard deviation of the neutral (thin line) and acidic pH (thick line) implicit solvent simulations. Average radius of gyration in seven of the acidic pH trajectories is 7.5 Å similar to the average radius of gyration of the coil structures at neutral pH is 7.2 Å. In the three other acidic trajectories, the average radius is larger, 8.5 Å. The upper and the lower values of the *x*-coordinate indicate the neutral and acidic pH simulation numbers, respectively.

observations regarding PrP106–126 at acidic pH, 10 simulations (10-ns each) (simulations 25–34 in Table I) were performed using the EEF1 implicit solvent model.[27] The average of the His^{111}–Val^{122} distance and of its standard deviation in these 10 trajectories is shown in Figure 16. These trajectories may be roughly sorted into two groups. A group of seven trajectories in which the average His^{111}–Val^{122} distance is 6.8 Å and a group of three trajectories in which the average His^{111}–Val^{122} distance is 12.6 Å. To further characterize the effect of the acidic pH on the compactness of the peptide the average radius of gyration for each of the 10 implicit solvent simulations at neutral and the 10 implicit solvent simulations at acidic pH are shown in Figure 17. As can be seen, the average radius of gyration of the coil structures at neutral pH is 7.2 Å. The average radius of gyration for the first group of seven acidic pH trajectories is 7.5 Å similar to the value at neutral pH. In the second group of the three trajectories with a larger His^{111}–Val^{122} distance the average radius of gyration is 8.5 Å. Thus, in some cases lowering the pH destabilizes the β-hairpin structure as reflected by the fluctuations in the β-hairpin stabilizing hydrophobic interactions and by the larger radius of gyration.

Figure 18 exhibits five snapshots of the peptide at acidic pH taken at 0.25-ns intervals along the 1-ns explicit solvent trajectory. The structures demonstrate that the hydrophobic interaction His^{111}–Val^{122} is weaker at acidic pH than those at neutral pH (Fig. 8). Because of the destabilization of intramolecular interactions at acidic pH, the peptide becomes more flexible and, consequently, it adopts conformations that are unlikely at neutral pH. A joint 2D projection of the two explicit solvent trajectories created at acidic and neutral pH is shown in Figure 19. This projection clearly shows that at acidic pH, the trajectory occupies a much larger conformation volume in comparison with the trajectory at neutral pH, despite the fact that the latter is twice as long than the former. This indicates that the destabilization of the hydrophobic interactions, resulting from the histidine protonation, enables the peptide to adopt conformations that are unlikely at neutral pH. The RMSD between the initial two β-sheet conformations is 1.70 Å. As the simulation proceeds, the RMSD between the structure of the two trajectory increases and becomes 5.28 Å at the end of the simulation.

CONCLUSIONS

In this study, we have carried out 34 MD simulations totaling 305 ns of simulation time (using both implicit and explicit solvent models) to study the helix-coil transition of a key prion fragment, PrP106–126, that is believed to include the region which is associated with the overall conformational transition characteristic of the full prion protein. The simulations were designed to explore the interactions that stabilize the α-helical and β-sheet conformations of the wild-type peptide and the mechanism by which the helix dissociates. Furthermore, the effects of a characteristic A117V mutation and the effect of acidic pH were also investigated. In general, the simulations, presented here agree with most of the experimental data accumulated in recent years, and supplies atomic-level molecular insight into the conformational conversion of the toxic amyloidogenic PrP106–126. This insight may help in developing approaches toward the prevention and treatment of amyloid fibril formation.

The simulations clearly show that in water at 300 K and neutral pH, the α-helix conformation of the PrP106–126 peptide is rather unstable. Starting from an α-helical conformation the peptide loses its helix structure in a short time (1.5 ns in explicit solvent and 4.3 ns in implicit solvent) adopting instead a random-coil conformation. In fact, this process is so fast that the loss of helicity starts as early as 0.5 ns after the beginning of the explicit solvent simulation. A comparison between the wild-type peptide and its A117V mutant, which is associated with the Gerstmann–Sträussler–Scheinker disease, showed that

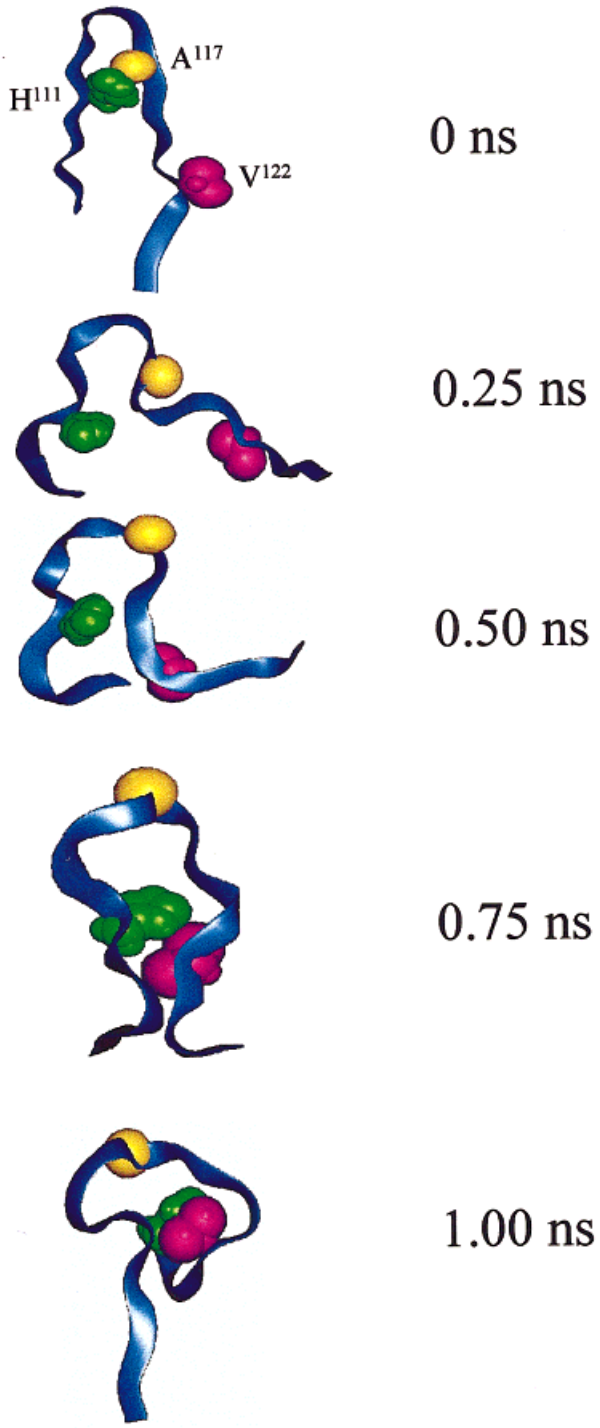

Fig. 18. Same as Fig. 8, but for the explicit solvent simulation of the wild-type peptide in acidic pH (simulation 4). The structures demonstrate that the hydrophobic interaction His^{111}–Val^{122} is weaker at acidic pH than those at neutral pH (Fig. 8) increasing the flexibility of the peptide.

this process of helix destabilization is even faster for the mutant peptide. In explicit solvent, the mutant peptide loses all traces of the initial helix structure within 0.5 ns; compared with the 1.5 ns, it takes the wild-type peptide to undergo the conversion into the coil structure. Likewise, in

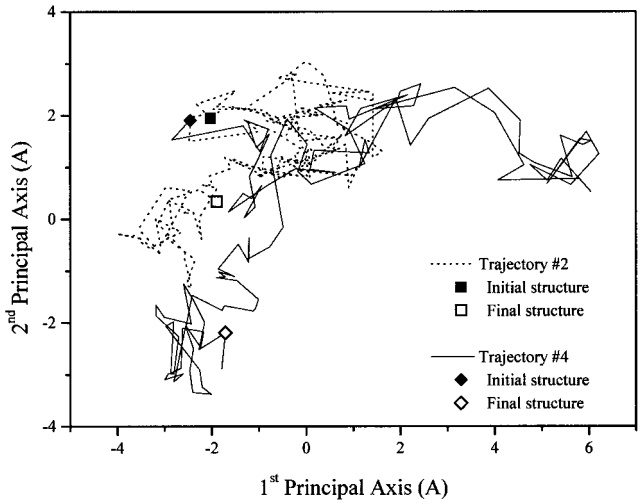

Fig. 19. Joint 2D projections of the explicit solvent trajectories created at acidic and at neutral pH (simulations 2 and 4). The root-mean-square deviation (RMSD) between the initial two β-sheet conformations is 1.70 Å. As the simulation proceeds, the RMSD between structure of the two trajectory increases and becomes 5.28 Å at the end of the simulations. The PrP106–126 trajectory at acidic pH occupies larger conformation volume compared with the equivalent trajectory at neutral pH.

implicit solvent, on average the mutant loses its initial helical structure within 2.8 ns, compared with 4.3 ns for the wild-type peptide. This observation helps explain the tendency of the A117V mutant prion protein to undergo a structural transition that results in a disease.

Furthermore, comparison between the wild-type and the A117V mutant demonstrates that not only is the rate of the helix-coil conversion affected by the mutation, but the mechanism as well. In the wild-type, the initial α-helix started to break up in the middle, near residues Ala^{114} and Ala^{115}, forming two smaller helices. This is followed by unwinding of the N-terminus fragment and can be viewed as the first step toward the formation of a β-hairpin stabilized by hydrophobic interactions. By contrast, the A117V mutant PrP106–126 begins to break up at the C-terminus region and then follows a gradual unwinding that ends with a disruption of the hydrogen bonds in the N-terminus region of the peptide. The difference can be attributed to the fact that the C-terminus region of the PrP106–126 is inherently unstable due to the Val residues 121 and 122, and the introduction of another Val through the A117V mutation lead to further instability of the helix. To conduct a more detailed study of the effect of the A117V mutation on the structure and the stability of PrP106–126, one may extend the simulations for chimeras that retain some of the properties of the amino acid found to play an important role in the unfolding process of the peptide.

The simulations reported in the present study also suggest that the helix-coil transition of both wild-type and mutant PrP106–126 is governed by the hydrophobic interaction between His^{111} and Val^{122}, rather than by the interaction between His^{111} and the residue at position 117 (whether Ala or Val). Therefore, the speedup of the α-helix breaking up by the A117V mutation is not due to a

formation of a stronger hydrophobic interaction with His^{111}, but rather due to an additional hydrophobic interaction, which does not exist in the normal peptide, between Val^{117} and Met^{112}. Interestingly, Met^{112} was recently found to be one of the two PrP104–113 determinants that interact with its antibody.[32]

As expected, a comparison between the simulation of the wild-type peptide at neutral pH and at acidic pH showed that at acidic pH, the stability of the stabilizing hydrophobic interaction (which we find to be His^{111}–Val^{122}) is reduced because of the protonation of the histidine. Consequently, the peptide became more flexible and adopted a broader range of coil conformations.

It should be noted that the instability of the α-helical conformation of PrP106–126 is not unique to this prion fragment. It has long been known that individual protein fragments or short polypeptide do not tend to form helices in water.[33] For instance, MD simulations have shown that the structure of polyalanine, which may be expected to be an α-helical conformation based on the highest α-helical propensity of alanine, is dependent on the chemical environments.[34,35] Accordingly, polyalanine is expected to adopt an α-helical conformation in nonpolar organic solvents and β-structures with coil conformations in a polar aqueous solution.[36] Furthermore, it was recently suggested that the changing properties of the peptide bond with the microenvironment affect helix-coil transitions as well.[37,38] MD simulations have shown that the unfolding time of various polypeptides, which are initially fully α-helical, is on the order of 0.3–2 ns,[39] in agreement with the observations of the present study. Hence, the uniqueness of the prion protein fragment PrP106–126 is not in the fact that it undergoes a rapid helix-coil conformational transition in aqueous solution but rather its the capability to self-assemble.

Our results suggest that the monomeric PrP106–126 is flexible in water and contains a random-coil structure with an overall loop shape. It is possible that a longer simulation is required to find the stable monomeric state of the PrP106–126, if such a single state exists. Alternatively, the peptide should be considered inherently flexible. Only when the aggregation commences does its flexibility reduce and the monomeric random-coil structure changes to a β-strand conformation or to a β-hairpin conformation. Salmona et al.[22] previously proposed that the monomeric PrP106–126 is a β-strand conformation. However, a β-hairpin conformation is also in agreement with their evidence that a positive charged C-terminus increases the fibrillogenic ability.

ACKNOWLEDGEMENT

Y. L. wishes to thank the support of Clore foundation.

REFERENCES

1. Prusiner SB. Molecular biology of prion diseases. Science 1991;252: 1515–1522.
2. Prusiner SB, Scott MR, DeArmond SJ, Cohen FE. Prion protein biology. Cell 1998;93:337–348.
3. James TL, Liu H, Ulyanov NB, Farr_Jones S, Zhang H, Donne DG, Kaneko K, Groth D, Mehlhorn I, Prusiner SB, Cohen FE. Solution structure of a 142-residue recombinant prion protein corresponding to the infectious fragment of the scrapie isoform. Proc Natl Acad Sci USA 1997;94:10086–10091.
4. Zhang H, Stockel J, Mehlhorn I, Groth D, Baldwin MA, Prusiner SB, James TL, Cohen FE. Physical studies of conformational plasticity in recombinant prion protein. Biochemistry 1997;36: 3543–3553.
5. Forloni G, Angorolli N, Chiosa R, Monzani E, Salmona M, Bugiani O, Tagliavini F. Neurotoxicity of a prion protein fragment. Nature 1993;362:543–546.
6. Riek R, Hornemann S, Wider G, Billeter M, Glockshuber R, Wuthrich K. NMR structure of the mouse prion protein domain Prp(121–231). Nature 1996;382:180–182.
7. Riek R, Hornemann S, Wider G, Glockshuber R, Wuthrich K. NMR characterization of the full-length recombinant murine prion protein. FEBS Lett 1997;413:282–288.
8. Caughey BW, Dong A, Bhat KS, Ernst D, Hayes SF, Caughey WS. Secondary structure analysis of the scrapie associated protein PrP27–30 in water by infrared spectroscopy. Biochemistry 1991;30: 7672–7680.
9. Pan KM, Baldwin M, Nguyen J, Gasset M, Serban A, Groth D, Mehlhorn I, Huang Z, Fletterick RJ, Cohen FE, Prusiner SB. Conversion of α-helices into β-sheets features in the formation of the scrapie prion proteins. Proc Natl Acad Sci USA 1993;90:10962–10966.
10. Inouye H, Kirschner DA. Folding and function of the myelin proteins from primary sequence data. J Neurochem Res 1991;28: 1–17.
11. Heller J, Kolbert AC, Larsen R, Ernst M, Bekker T, Baldwin M, Prusiner SB, Pines A, Wemmer DE. Solid-state NMR studies of the prion protein H1 fragment. Protein Sci 1996;5:1655–1661.
12. Donne DG, Viles JH, Groth D, Mehlhorn I, James TL, Cohen FE, Prusiner SB, Wright PE, Dyson HJ. Structure of the recombinant full-length hamster prion protein PrP (29–231): the N terminus is highly flexible. Proc Natl Acad Sci USA 1997;94:13452–13457.
13. Zahn R, Liu A, Lührs T, Riek R, Von Schroetter C, Garcia L, Billeter M, Calzolai L, Wider G, Wüthrich K. NMR solution structure of the human prion protein. Proc Natl Acad Sci USA 2000;97:145–150.
14. Gasset M, Baldwin MA, Lloyd D, Gabriel JM, Holtzman DM, Cohen FE, Gletterick R, Prusiner SB. Predicted alphα-helical regions of the prion protein when synthesized as peptides form amyloid. Proc Natl Acad Sci USA 1992;89:10940–10944.
15. Nguyen JT, Baldwin MA, Cohen FE, Prusiner SB. Prion protein peptides induce alphα-helix to beta-sheet conformational transitions. Biochemistry 1995;34:4186–4192.
16. Blondelle SE, Forood B, Houghten RA, Pérez-Payá E. Polyalanine-based peptides as models for self-associated β-pleated-sheet complexes. Biochemistry 1997;36:8393–8400.
17. Inouye H, Kirschner DA. Polypeptide chain folding in the hydrophobic core of hamster scrapie prion: analysis by x-ray diffraction. J Struct Biol 1998;122:247–255.
18. Brown DR, Schmidt B, Kretzschmar HA. Role of microglia and host prion protein in neurotoxicity of a prion protein fragment. Nature 1996;380:345–347.
19. Selvaggini C, De Gioia L, Cantu L, Ghibaudi E, Diomede L, Passerini F, Forloni G, Bugiani O, Tagliavini F, Salmona M. Molecular characteristics of a protease-resistant, amyloidogenic and neurotoxic peptide homologous to residues 106–126 of the prion protein. Biochem Biophys Res Commun 1993;194:1380–1386.
20. De Gioia L, Selvaggini C, Ghibaudi E, Diomede L, Bugiani O, Forloni G, Tagliavini F, Salmona M. Conformational polymorphism of the amyloidogenic and neurotoxic peptide homologous to residues 106–126 of the prion protein. J Biol Chem 1994;269:7859–7862.
21. Muramoto T, Scott M, Cohen FE, Prusiner SB. Recombinant scrapie-like prion protein of 106 amino acids is soluble. Proc Natl Acad Sci USA 1996;93:15457–15462.
22. Salmona M, Malesani P, De Gioia L, Gorla S, Bruschi M, Molinari A, Della Vedova R, Pedrotti B, Marrari MA, Awan T, Bugiani O, Forloni G, Tagliavini F. Molecular determinants of the physicochemical properties of a critical prion protein region comprising residues 106–126. Biochem J 1999;342:207–214.
23. Ragg E, Tagliavini F, Malesani P, Monticelli L, Bugianim O, Forloni G, Salmona M. Determination of solution conformations of PrP106–126, a neurotoxic fragment of prion protein, by 1H NMR

and restrained molecular dynamics. Eur J Biochem 1999;266:1192–1201.
24. Kazmirski SL, Alonso DOV, Cohen FE, Prusiner SB, Daggett V. Theoretical studies of sequence effects on the conformational properties of a fragment of the prion protein: implications for scrapie formation. Chem Biol 1995;2:305–315.
25. Brooks BR, Bruccoleri RE, Olafson BD, States DJ, Swaminathan S, Karplus M. CHARMM: a program for macromolecular energy, minimization and dynamic calculation. J Comput Chem 1983;4: 187–217.
26. MacKerell AD Jr, Bashford D, Bellot M, Dunbrack RL Jr, Evanseck JD, Field MJ, et al. All-atom empirical potential for molecular modeling and dynamics studies of proteins. J Phys Chem B 1998;102:3586–3616.
27. Lazaridis T, Karplus M. Effective energy function for proteins in solution. Proteins 1999;35:133–152.
28. Lazaridis T, Karplus M. "New view" of protein folding reconciled with the old through multiple unfolding simulations. Science 1997;278:1928–1931.
29. Kabsch W, Sander C. Dictionary of protein secondary structure: pattern recognition of hydrogen-bonded and geometrical features. Biopolymers 1983;22:2577–2637.
30. Becker OM. Principal coordinate maps of molecular potential energy surfaces. J Comp Chem 1998;19:1255–1267.
31. Becker OM, Levy Y, Ravitz O. Flexibility, conformation spaces, and bioactivity. J Phys Chem 2000;104:2123–2135.
32. Kanyo ZF, Pan KM, Williamson RA, Burton DR, Prusiner SB, Fletterick RJ, Cohen FE. Antibody binding defines a structure for an epitope that participates in the PrP^{C} (PrP^{SC} conformational change. J Mol Biol 1999;293:855–863.
33. Zimm BH, Bragg JK. Theory of the phase transition between helix and random coil. J Chem Phys 1959;31:526–535.
34. Daggett V, Levitt M. Molecular dynamics simulations of helix denaturation. J Mol Biol 1992;223:1121–1138.
35. Takano M, Yamato T, Higo J, Suyama A, Nagayama K. J Am Chem Soc 1999;121:605–612.
36. Levy Y, Jortner J, Becker OM. Solvent effects on the energy landscapes and folding kinetics of polyalanine. Proc Natl Acad Sci USA 2001;98:2188–2193.
37. Rick SW, Cachau RE. The nonplanarity of the peptide group: molecular dynamics simulations with a polarizable two-state model for the peptide bond. J Chem Phys 2000;112;5230–5241.
38. Buck M, Karplus M. Internal and overall peptide group motion in proteins: molecular dynamics simulations for lysozyme compared with results from x-ray and NMR spectroscopy. J Am Chem Soc 1999;121:9645–9658.
39. Doruker P, Bahar I. Role of water on unfolding kinetics of helical peptides studied by molecular dynamics simulations. Biophys J 1997;72:2445–2456.